IOP Conference Series: Materials Science and Engineering

PAPER • OPEN ACCESS

Influence of the wear rings on the buckling behaviour of hydraulic actuators

To cite this article: E V Arcieri and S Baragetti 2023 *IOP Conf. Ser.: Mater. Sci. Eng.* **1275** 012029

IOP Conf. Series: Materials Science and Engineering 1275 (2023) 012029 doi:10.1088/1757-899X/1275/1/012029

Influence of the wear rings on the buckling behaviour of hydraulic actuators

E V Arcieri[1] and S Baragetti[1]

[1]Department of Management, Information and Production Engineering, University of Bergamo, Viale Marconi 5, Dalmine 24044, Italy

sergio.baragetti@unibg.it

Abstract. During their use, hydraulic actuators are generally subjected to compressive loads which can induce buckling. In this work the critical load of a hydraulic actuator was determined for various boundary conditions and types of wear rings by theoretical and numerical models. In the theoretical model, the actuator was modelled as two connected beams, with different sections. The contribution of the wear rings on the critical load of the actuator was determined through numerical simulation based on the finite element method. The results of the mathematical model are similar to the results provided by the finite element analyses. The contribution of the investigated wear rings stiffness is very low for the materials considered for these components in this paper.

1. Introduction

Hydraulic actuators are commonly used in civil and industrial applications to apply forces. They have low construction and operation costs, reduced size and great strength. A hydraulic actuator mainly consists of two parts, a cylinder and a rod. Wear rings are typically mounted at the rod-cylinder connection in the gland and in some cases also between the external surface of the piston and the internal surface of the cylinder. The purpose of the wear rings is to guide the rod and piston, with reduced friction and improved sealing quality.

Due to their configuration, hydraulic actuators are commonly subjected to compression during their use with a consequent risk of buckling, which is one of the most common causes of failure in mechanical systems, in addition to the presence of stress concentrations [1], corrosion [2] and fatigue [3].

The bending and buckling behaviour of hydraulic actuators has only been studied in more detail since the second half of the 1900s, starting from Euler's method. Early mathematical models considered the buckling behaviour of a single beam. In [4] the device was modelled as a single beam with rod inertial properties over the entire length of the hydraulic actuator. This approximation leads to underestimate the real strength of the system. In [5] the system was modelled as a two-beam structure, with a rod and an infinite stiffness hollow cylinder, with a consequent overestimation of the actual load capacity of the actuator. Timoshenko and Gere [6] adopted a model with two different sections for rod and cylinder to consider their different moment of inertia. In [7, 8] it was shown that the presence of the fluid inside the actuator does not influence the critical load. In [9] the geometrical imperfections of the system that can cause premature deformations were examined. In fact, rectilinear imperfections induce an eccentricity of the load and a further bending moment. Ravinshankar [10] applied the finite element method to investigate the stress state in a hydraulic cylinder by modelling the system as an assembly of space frame elements. The contribution of the bearings and seals at the rod-cylinder interface was modelled with a rotary spring. Yoo and Siegel [11] estimated the critical column loads on telescopic power cylinders. They also considered the influence of support conditions and lateral load. In [12, 13] the influence of rectilinear imperfections was investigated analytically. Gamez-Montero and coauthors [14] considered the influence of the own weight of the actuator and fluid pressure on the buckling behaviour. The results confirmed the negligible effects of pressure, as found in [7, 8], and the validity of the analytical models in [12, 13]. Friction moments in the joint of the end supports were identified as critical for the load capacity of the actuators in [15]. In [16], the finite element method was used to conduct a sensitivity analysis in order to identify the effects of rectilinear imperfections and friction in the supports on the limit buckling load of the actuators. Zhou and coauthors [17] stress the need to consider large deflection and shear effect and bending stiffness of cylinder-rod joint in the models which describe the buckling behaviour of a horizontal hydraulic cylinder articulated at both supports. Taking into consideration the results above, the methods for evaluating the buckling load of hydraulic cylinders presented in the ISO/TS 13725:2021 standard [18] are based on the elastic buckling theory and consider the possible off-axis loading and the weight of the system.

In this work the critical buckling load of a hydraulic actuator was calculated considering different boundary conditions and types of wear rings [19]. The buckling load of the actuator was calculated using theoretical and numerical models. The presented theoretical model considers the actuator as two connected beams. Finite element analysis was used to determine the influence of the wear rings on the critical load of the whole system. The results of the mathematical and numerical models are similar and show that the influence of the investigated wear ring materials on the critical load of the actuator is limited.

2. Data for the analyses

For the study, the actuator of Figure 1 [12, 13, 16] was considered. It consists of a rod, a cylinder, a gland, a piston and four wear rings. Two wear rings are mounted at the rod-cylinder connection in the gland and two are mounted between the external surface of the piston and the internal surface of the cylinder. In the models presented in this work, the presence of the piston and the gland was not modelled. The rod and the cylinder were considered made of steel S235. Four types of wear rings were analysed, WR1, WR2, WR3 and WR4. WR1 and WR2 were commercial while WR3 and WR4 were fabricated using fused deposition modelling additive manufacturing process. Table 1 [12, 13, 16] summarizes the geometrical and mechanical properties of the hydraulic actuator components.

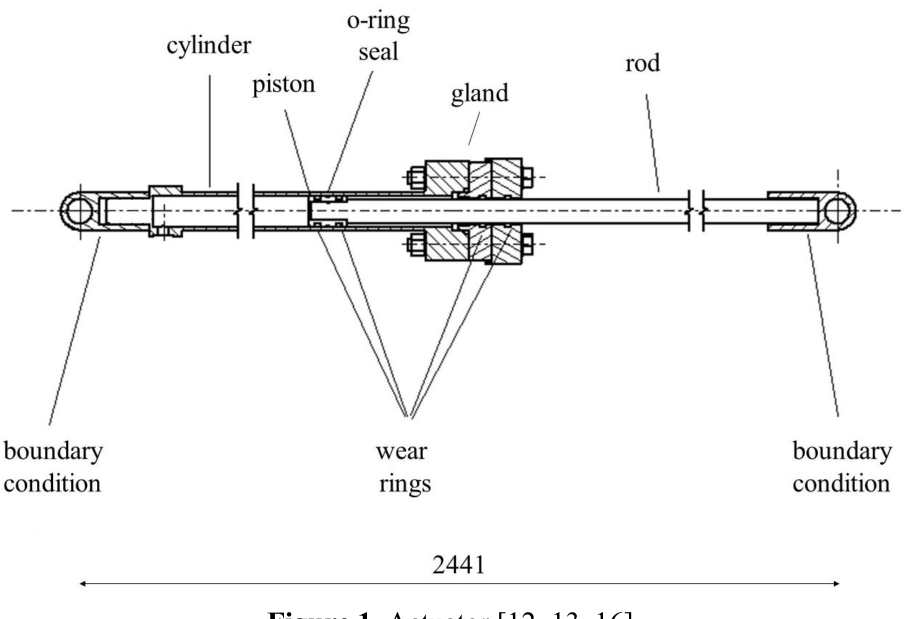

Figure 1. Actuator [12, 13, 16].

Table 1. Data [12, 13, 16].

Property	Value
Rod diameter (mm)	20
Cylinder external diameter (mm)	30
Cylinder internal diameter (mm)	25
Rod length (mm)	1165
Cylinder length (mm)	1276
Wear ring external diameter (mm)	25
Wear ring internal diameter (mm)	20
Wear ring height (mm)	5
Rod and cylinder Young's modulus – steel S235 (MPa)	206000
Rod and cylinder Poisson's ratio – steel S235	0.3
Rod and cylinder density – steel S235 (kg/m^3)	7850
WR1 Young's modulus – polyamide (MPa)	3000
WR2 Young's modulus – composite (MPa)	600
WR3 Young's modulus – polylactide (MPa)	2347
WR4 Young's modulus – nylon (MPa)	579
Wear ring Poisson's ratio	0.3

3. Mathematical model

The research method applied in this paper is the same one adopted in [20, 21]. Considering the equilibrium of an infinitesimal element of a beam, it is possible to obtain Equation 1:

$$\frac{d^4u}{dz^4} + \alpha^2 \frac{d^2u}{dz^2} = 0, \alpha^2 = N/EI \tag{1}$$

where u is the displacement in the direction normal to the axial direction z, N the axial load, E the Young's modulus of the material and I the section moment of inertia.

Equation 1 is a fourth-order differential equation whose associated homogeneous solution is defined by Equation 2:

$$u(z) = A\cos(\alpha z) + B\sin(\alpha z) + Cz + D \tag{2}$$

In the mathematical model, the actuator was modelled as two connected beams, one with a solid section (rod) and the other with a hollow section (cylinder) based on the geometry of the hydraulic actuator described in Section 2. Equation 2 was written for both the rod and the cylinder. Ground boundary conditions were modelled, namely pinned-pinned, fixed-pinned and fixed-fixed. The continuity of transversal displacement, rotation, bending moment and shear was set to model the fixed support between the two beams. The parameter to be obtained through the solution of the problem was the critical load N_{cr}, which is included in the terms α_{rod} and $\alpha_{cylinder}$ that appear when Equation 2 is written for the rod and the cylinder respectively. By assuming $\alpha_{cylinder} = \beta\alpha_{rod}$ ($\beta = (I_{rod}/I_{cylinder})^{0.5}$, where I_{rod} is the moment of inertia of the rod and $I_{cylinder}$ the moment of inertia of the cylinder), it is possible to solve the system of Equation 3 with respect to the variable α_{rod}:

$$[X]\,[Y] = [0] \tag{3}$$

where [X] represents the matrix of the coefficients, [Y] the vector of unknowns and [0] the vector of the known terms (null vector). The first solution with physical meaning of the system in Equation 3 is the critical load of the actuator and can be found by imposing det[X] = 0.

4. Finite element analyses

Under normal conditions of use, the deformation of the wear rings could influence the actuator critical load. If worn or overloaded, the wear rings may no longer be able to keep the rod aligned with the cylinder. In this case, the applied load would become eccentric with respect to the axis of the actuator, with consequent possible reduction of buckling load. Finite element analyses were conducted to calculate the radial stiffness of the wear rings and the critical load of the actuator for the different types of wear rings investigated.

4.1. Model for determining the radial stiffness of the wear rings

Given the geometry of each wear ring and the material with which it was made, a 3D finite element analysis was conducted on the model of a half of the wear ring with the Abaqus/Standard code [22] to determine its radial stiffness. The model is shown in Figure 2. The wear ring was modelled with solid elements. The load on the wear ring was applied by a semi-cylindrical surface, concentric with the wear ring. Each node of this surface was rigidly connected to a reference point (RP) positioned on the axis of the wear ring. The nodes on the outer surface of the wear ring were prevented from moving in the radial direction. A concentrated load was applied at the RP. The load direction was radial with respect to the wear ring and on the symmetry plane. Symmetry boundary conditions were set. The maximum displacement in the load direction was measured to determine the radial stiffness of the wear ring.

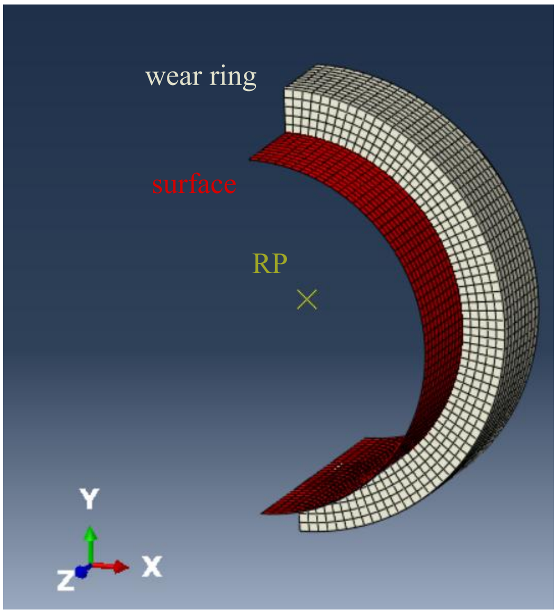

Figure 2. Finite element model for the calculation of the radial stiffness of the wear rings.

4.2. Model for determining the critical load of the actuator

To calculate the critical load of the actuator with different boundary conditions and types of wear rings, a 3D buckling analysis was conducted in Abaqus [22]. For the analysis, the cylinder, the rod and the wear rings were modelled. Shell elements were used to model the cylinder and beam elements were used to model the rod. The mechanical properties of steel S235 were assigned to the cylinder and rod. Two perpendicular linear elastic elements were used to model each wear ring in the actuator (Figure 3). The stiffness calculated with the procedure described in the previous section was assigned to the elastic elements.

IOP Conf. Series: Materials Science and Engineering 1275 (2023) 012029 doi:10.1088/1757-899X/1275/1/012029

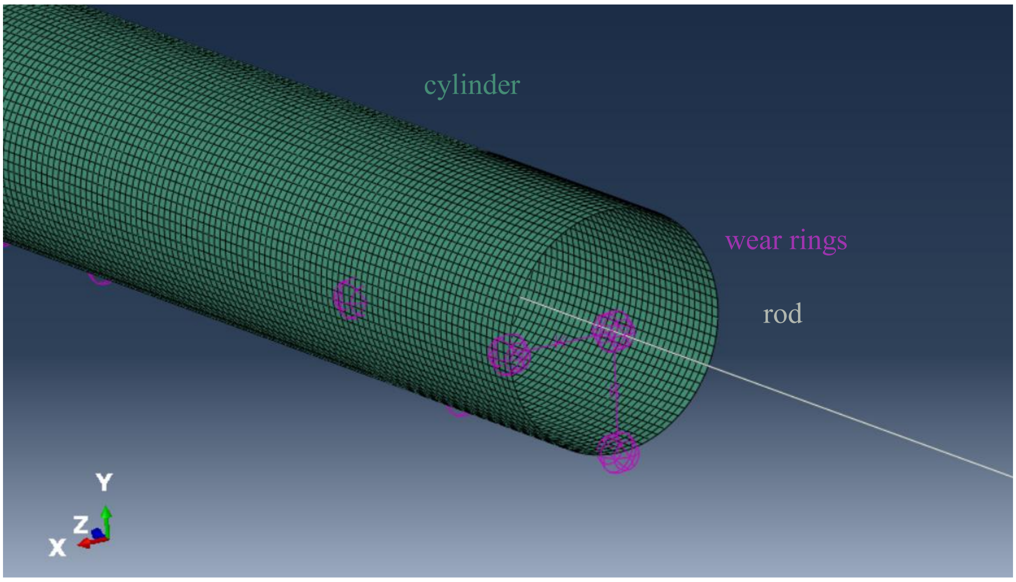

Figure 3. Finite element model for the calculation of the critical load, detail.

The fluid in the actuator was considered incompressible. To simulate this condition, the rod and cylinder were coupled with a coupling constraint and all the degrees of freedom of the coupling nodes were constrained except for the translation on the plane perpendicular to the axis of the actuator. The nodes at the end of the cylinder were rigidly connected to a RP placed in the centre of the section. Different boundary conditions were applied to this RP and to the node placed at the end of the rod. In the latter node the movement in the axial direction of the actuator was always left free. In this direction an arbitrary concentrated load was assigned. The arbitrary load, multiplied by the first critical multiplier obtained with the finite element method, is the buckling critical load of the actuator.

5. Results and discussion

Table 2 shows the values of critical load obtained with the mathematical and numerical models described in the previous sections.

Table 2. Results of the mathematical and numerical models.

Critical load [kN]	Pinned-pinned	Fixed-pinned	Fixed-fixed
Mathematical model	3.9	7.5	15.6
Numerical model, WR1	4.0	7.7	16.0
Numerical model, WR2	3.9	7.7	15.9
Numerical model, WR3	4.0	7.7	16.0
Numerical model, WR4	3.9	7.7	15.9

According to the results of the numerical models, the four types of wear ring investigated provide very similar values of critical load. The mounting of WR1 globally induces the maximum value of critical load for the actuator, while the mounting of WR4 provides the minimum value. WR1 is the stiffest wear ring of the four types investigated and WR4 is the least stiff (Table 1).

For all the three boundary conditions analysed, the theoretical results are similar to the numerical ones. The discrepancies between the results provided by the theoretical model and the finite element analyses are a few percentage points.

As expected, the critical load increases as the boundary conditions become stricter (the effective length factor becomes smaller), with the highest values of buckling critical load obtained for the fixed-fixed boundary condition.

6. Conclusions and future developments

In this work the critical buckling load of a hydraulic actuator was calculated for different boundary conditions and types of wear rings using theoretical and finite element models. In the theoretical model, the system was modelled as two connected beams. Finite element analyses were conducted on a model of the system containing the rod, the cylinder and the wear rings. The results of the mathematical model and finite element analyses are similar. The contribution of the wear rings stiffness is very low for the materials considered in this paper. An experimental test campaign will be planned to validate the obtained results. Some of the wear rings considered in this study were produced by additive manufacturing. Since the dimensional and geometrical tolerances obtained with this technology are poor, it would be interesting to determine how geometrical tolerances of wear rings influence the buckling behaviour of the actuator.

References

[1] Baragetti S, Borzini E and Arcieri E V 2018 *Procedia Struct. Integr.* **12** 173-182
[2] Srinivasan N, Bhaskar L K, Kumar R and Baragetti S 2018 *Mater. Des.* **160** 303-312
[3] Baragetti S and Baryshnikov A 2001 *J. Mech. Design* **123** 456-463
[4] Bleich F 1952 *Buckling Strength of Metal Structures* (New York: McGraw-Hill)
[5] Belluzzi O 1961 *Scienza delle Costruzioni* (Bologna: Zanichelli)
[6] Timoshenko S P and Gere J M 1961 *Theory of Elastic Stability* (Tokyo: McGraw-Hill)
[7] Flügge W 1973 *Stresses in Shells* (Berlin: Springer)
[8] Hoblit F 1950 *Prod. Eng.* **21** 108–112
[9] Seshasai K, Dawkins W and Iyengar S 1975 *Proc. Natl. Conf. Fluid Power*
[10] Ravishankar N 1981 *J. Mech. Des.* **103** 239-243
[11] Yoo C H and Siegel C R 1986 *Comput. Struct.* **22** 245-251
[12] Baragetti S and Terranova A 1999 *Int. J. Mater. Prod. Technol.* **14** 50–73
[13] Baragetti S and Terranova A 2001 *Proc. Inst. Mech. Eng., Part C* **215** 607–619
[14] Gamez-Montero P J, Salazar E, Castilla R, Freire J, Khamashta M and Codina E 2009 *Int. J. Mech. Sci.* **51** 105–113
[15] Gamez-Montero P J, Salazar E, Castilla R, Freire J, Khamashta M and Codina E 2009 *Int. J. Mech. Sci*. **51** 145–151
[16] Baragetti S and Villa F 2016 *Math. Probl. Eng.* **2016** 3781397
[17] Zhou J, Shi D, Di C, Zhang Y and Cheng X 2020 *Int. J. Struct. Stab. Dyn.* **20** 2050033
[18] ISO/TS 13725:2021 Hydraulic fluid power — Method for evaluating the buckling load of a hydraulic cylinder
[19] Costanzo S 2021 Instabilità progressiva di attuatori idraulici: modelli teorici, numerici e risultati sperimentali (master thesis)
[20] Baragetti S 2006 *Meccanica* **41** 443-458
[21] Baragetti S and Arcieri E V 2019 *Procedia Struct. Integr.* **24** 91-100
[22] ABAQUS, ABAQUS Documentation, Dassault Systèmes, Providence, RI, USA, 2017